

Physics prospects at a linear e^+e^- collider

SAURABH D RINDANI

Theory Group, Physical Research Laboratory, Navrangpura, Ahmedabad 380 009, India
E-mail: saurabh@prl.res.in

Abstract. The talk described the prospects of studying standard model parameters as well as scenarios beyond the standard model, like the minimal supersymmetric standard model, theories with extra dimensions and theories with extra neutral gauge bosons, at a future linear e^+e^- collider.

Keywords. Linear collider; standard model; physics beyond the standard model.

PACS Nos 13.66.Jn; 13.66.Hk; 13.66.Fg

1. Introduction

1.1 *The need for an e^+e^- collider*

The large hadron collider (LHC) colliding protons on protons at a centre-of-mass (cm) energy of 14 TeV will become operational next year. It will look for the Higgs boson, the missing link of the standard model (SM), and also for new physics beyond the standard model (BSM). However, while LHC will be a good tool to discover new physics, it is generally realized that for precision measurements of parameters of various theories, there is need for a high luminosity e^+e^- collider operating at a cm energy of at least a few hundred GeV [1]. It would thus be complementary to hadronic colliders.

An inherent advantage of an e^+e^- collider is a smaller hadronic background. Hence, higher accuracy for a lower energy is possible. Here it is appropriate to recall the success of LEP in making precise measurements of the couplings of the Z and other SM parameters. Another advantage of an e^+e^- collider is that the energy of the incoming particles is fixed and tunable, unlike the energies of partons participating in a hadronic collision.

The other advantage of a linear collider is that there is the possibility of having $\gamma\gamma$, γe and e^-e^- as additional modes, which can provide qualitatively and quantitatively different information. A further option known as the GigaZ option can be used to improve on the accuracy of LEP with the use of a higher luminosity with the energy tuned to the Z resonance.

1.2 Features of an e^+e^- collider

1.2.1 Parameters of the collider

The centre-of-mass (cm) energy of the linear collider would range from 300 to 1000 GeV. It would be expected to operate just above the $t\bar{t}$ threshold for the study of the top mass, and at $\sqrt{s} = 500$ GeV for most of the remaining data. Studies show that it would be useful to operate it at a higher cm energy like 800 or 1000 GeV at a higher luminosity for studying certain processes. The expected luminosity is a few times 10^{34} $\text{cm}^{-2} \text{s}^{-1}$ at 500 GeV, which is equivalent to an integrated luminosity of 500 fb^{-1} after a run of a couple of years or so. As mentioned earlier, it may be operated at $\sqrt{s} = m_Z$ (GigaZ option). It seems possible to have a high degree of longitudinal beam polarization for e^- as well as e^+ . An International Technology Recommendation Panel took a decision that the collider would be built based on 'cold' (superconducting) technology, rather than 'warm' (room temperature) technology.

1.2.2 Options at the ILC

A number of options have been suggested for ILC. First of all, it could be run in e^+e^- or e^-e^- modes. This would realize qualitatively different physics goals. There could also be quantitative differences on account of different backgrounds in the two cases.

The other kind of option arises because the beams can be polarized. e^- as well as e^+ beams could be longitudinally polarized, though the technologies in the two cases are different. The anticipated e^- polarization is 80–90%, whereas the anticipated e^+ polarization is around 60%. Longitudinally polarized beams can help to reduce background as well as improve sensitivity [2]. While for many purposes the presence of e^- polarization alone helps, the availability of e^+ polarization at the same time is essential for some processes [2]. In the case of longitudinal polarization, the effective polarization for most processes is the combination

$$P_{\text{eff}} = (P_{e^-} - P_{e^+}) / (1 - P_{e^-} P_{e^+}). \quad (1)$$

This can be larger than individual polarizations, depending on their relative signs. It is nonzero, and equal to P_{e^-} even when e^+ polarization is zero.

It is also possible to convert longitudinal polarization to transverse polarization using spin rotators. Transverse polarization, through azimuthal distributions, helps to provide qualitatively different information as compared to longitudinal polarization [2].

It has been pointed out that Compton backscattering of high-intensity laser beams off high-energy electron beams can give photon beams which carry a large fraction of the electron energy [3,4]. Figure 1, taken from [3], shows the spectrum of photons expected from laser backscattering. It can be seen that if the product of the laser photon helicity P_c and the electron helicity λ_e is negative, the spectrum is highly peaked at a large value of the ratio y of the photon energy ω to

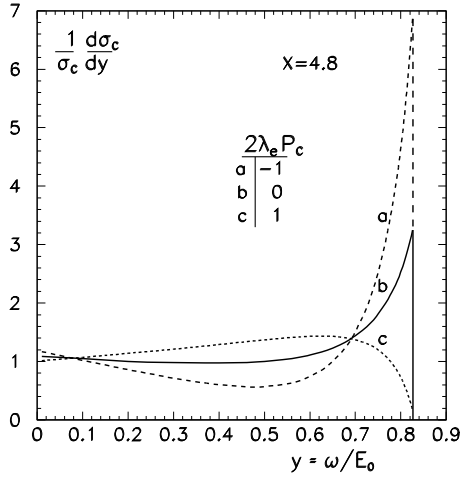


Figure 1. The spectrum of photons obtained by backscattering of a laser beam off high energy electrons (from [3]).

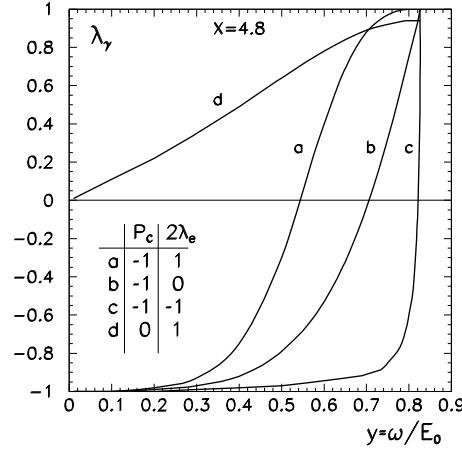


Figure 2. The polarization of photons produced by backscattering a polarized laser beam off polarized high energy electrons (from [3]).

the electron energy E_0 . Polarized laser and electron beams can give high degree of photon polarization for a certain choice of laser photon and electron polarizations, as shown in figure 2, taken from [3]. In addition it would also be possible to have $e^\pm\gamma$ collisions.

2. Standard model physics at the linear collider

2.1 Gauge-boson self-interactions

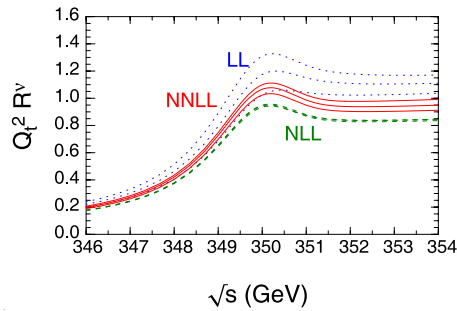
The primary goal of studying gauge-boson self-interactions is to establish the non-Abelian nature of electroweak interactions. Processes sensitive to triple-gauge couplings are $e^+e^- \rightarrow W^+W^-$ and $e^+e^- \rightarrow W^\pm e^\mp \nu$. These have already been studied at LEP2. In view of the much higher luminosity available at ILC, the accuracy of measurement would be greater. At high luminosity and with the help of beam polarization, triple gauge couplings can be determined with an error of a few $\times 10^{-4}$. The accuracy for different anomalous couplings is shown in table 1, taken from [5]. Neutral gauge boson anomalous couplings can be determined to the same precision in $e^+e^- \rightarrow \gamma Z, ZZ$. Asymmetries with longitudinal or transverse polarization can be used for CP-odd couplings [6].

2.2 Top-quark production at threshold

Top-quark mass measurement can be made in top-quark pair production in the threshold region. The top mass can be measured precisely from a scan of the $t\bar{t}$

Table 1. Limits on various anomalous couplings at ILC (from [5]).

	$\sqrt{s} = 500$ GeV	$\sqrt{s} = 800$ GeV
Δg_1^Z	15.5	12.6
$\Delta \kappa_\gamma$	3.3	1.9
λ_γ	5.9	3.3
$\Delta \kappa_Z$	3.2	1.9
λ_Z	6.7	3.0
g_5^Z	16.5	14.4
g_4^Z	45.9	18.3
$\tilde{\kappa}_Z$	39.0	14.3
$\tilde{\lambda}_Z$	7.5	3.0

**Figure 3.** Dependence of the $e^+e^- \rightarrow t\bar{t}$ cross-section on \sqrt{s} . The curves labelled LL (dotted), NLL (dashed), and NNLL (solid) include leading logarithmic, next-to-leading logarithmic, and next-to-next-to-leading logarithmic contributions, respectively. The three curves for each set of corrections represent the variation of the rate with changes of the renormalization scale. This figure uses a threshold mass definition for the top quark mass [9] (from [7]).

threshold ($\sqrt{s} \approx 340\text{--}380$ GeV). Theoretical analysis of the cross-section needs a double-expansion of $\sigma_{t\bar{t}}$ in α_s and $\beta = \sqrt{1 - 4m_t^2/s}$, the velocity of the top quark. Terms up to next-next-to-leading order (NNLO) have been calculated [7,8]. It is found that simultaneous precision measurement of m_t and α_s will be possible. Figure 3 shows the calculated cross-section for $e^+e^- \rightarrow t\bar{t}$ near the threshold in the leading logarithmic, next-to-leading logarithmic and next-to-next-to-leading logarithmic approximations, taken from [7], using a threshold mass definition for the top quark from [9]. With a 10-point scan, the expected precisions in the top mass, α_s , and the width of the top quark are, respectively, $\Delta m_t = 42$ MeV, $\Delta \alpha_s(M_Z) = 0.001$, $\Delta \Gamma_t = 50$ MeV. Including theoretical uncertainties, the precision expected is $\Delta m_t(\overline{MS}) = 100$ MeV [10].

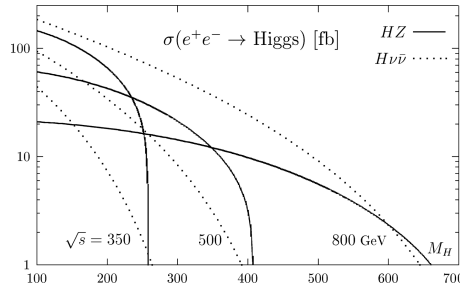


Figure 4. The Higgsstrahlung and WW fusion production cross-sections vs. the Higgs mass for $\sqrt{s} = 300$ GeV, 500 GeV and 800 GeV (from [11]).

2.3 Search for the SM Higgs boson

Search for the Higgs boson is of high priority at the LHC and the ILC. Once the Higgs is found, measuring its properties will be necessary for understanding the origin of gauge symmetry breaking and masses of various particles. To test the completeness of the minimal SM and the Higgs mechanism as the source of mass, measurements must show the following:

- Couplings of the Higgs boson to fermions and gauge bosons are proportional to their masses. This needs measurement of branching ratios.
- The Higgs boson has quantum numbers $J^{\text{CP}} = 0^{++}$.
- The Higgs boson is the source of its own mass. This needs the measurement of trilinear and quartic self-couplings.

The Higgs boson can be produced at a linear collider through ‘Higgsstrahlung’ (the Bjorken mechanism): $e^+e^- \rightarrow ZH$, WW fusion: $e^+e^- \rightarrow \nu_e\bar{\nu}_eH$, or ZZ fusion: $e^+e^- \rightarrow e^+e^-Z$. Figure 4 shows the production cross-sections for the former two processes. At $\sqrt{s} = 500$ GeV, Higgsstrahlung dominates for $m_H \lesssim 160$ GeV, whereas WW fusion dominates for $m_H \gtrsim 160$ GeV. For $\sqrt{s} = 800$ GeV, the dominant mechanism is WW fusion. ZZ fusion contributes 10% at $\sqrt{s} = 800$ GeV.

2.4 Measuring Higgs couplings

To distinguish the SM Higgs from the Higgs of an extended model it is necessary to measure Higgs couplings with precision. For this it is necessary to measure various decay branching ratios. Figure 5 shows the branching ratio and total width of a SM Higgs as a function of its mass.

For $m_H < 150$ GeV, $H \rightarrow b\bar{b}$ dominates. Coupling to the bottom quark can be determined to a precision of about 2%. Couplings to the charm quark and τ can be determined to a precision of about 12% [12]. Coupling to the muon is expected to be poorly measured, to about 30% [13].

The top quark, being much heavier than other quarks, can play a special role. For $m_H < 2m_t$, the Higgs coupling to the top can be measured through

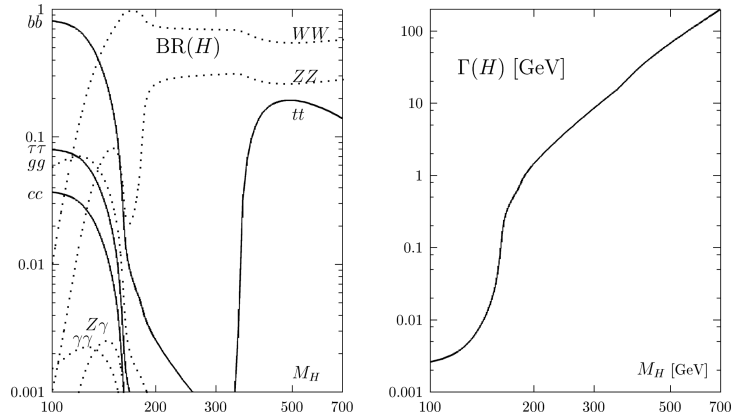


Figure 5. Branching ratios (left) and the total width (right) of the SM Higgs as a function of its mass (from [11]).

$$e^+e^- \rightarrow t\bar{t}H. \tag{2}$$

This suffers from small rate and requires higher energy and luminosity. For $\sqrt{s} \gtrsim 800$ GeV and $L \approx 1000 \text{ fb}^{-1}$, the Higgs coupling to the top can be measured to 10% accuracy [14].

2.5 Measurement of Higgs self-couplings

Higgs self-couplings in SM are described by the terms in the scalar potential:

$$V = \frac{1}{2}m_H^2 H^2 + \lambda_3 v H^3 + \frac{1}{4}\lambda_4 H^4. \tag{3}$$

To establish the correctness of these terms, one needs to check the relation:

$$\lambda_3 = \lambda_4 = m_H^2/(2v). \tag{4}$$

Measuring λ_3 (λ_4) requires the production of 2 (3) Higgs bosons through double (triple) Higgsstrahlung. For $\sqrt{s} = 500$ GeV, and an integrated luminosity of 1000 fb^{-1} , λ_3 can be determined to 20% accuracy through $e^+e^- \rightarrow ZHH$, $H \rightarrow b\bar{b}$, for $120 \text{ GeV} < m_H < 140 \text{ GeV}$ [15]. λ_4 is not easy to determine because of the small rate for $e^+e^- \rightarrow ZHHH$ [16].

2.6 Spin of the Higgs

For the SM Higgs it is necessary to verify that it has spin 0 and its CP even nature. The angular distribution of Z in $e^+e^- \rightarrow ZH$ for a $J^P = 0^+$ Higgs should be $d\sigma/d\cos\theta \sim \sin^2\theta$ [17]. The spin can be determined from the \sqrt{s} dependence of the cross-section σ [18]. Figure 6 shows the \sqrt{s} dependence of σ for the values 0, 1

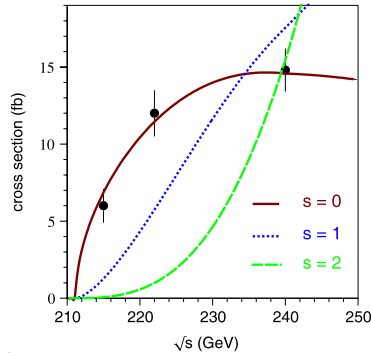


Figure 6. The dependence of the cross-section for Higgs production via $e^+e^- \rightarrow ZH$ for values of the Higgs spin $s = 0, 1$ and 2 (from [18]).

and 2 for the spin of the Higgs. The spin can be determined from the invariant mass of the virtual Z in the decay $H \rightarrow Z^*Z$ for $m_H < 2m_Z$. The angular distribution of decay products in $H \rightarrow Z^*Z$ can distinguish $P = +$ from $P = -$ [19]. These measurements are near the HZ threshold, and require low luminosity ($\sim 20 \text{ fb}^{-1}$). Finally, the observation of $H \rightarrow \gamma\gamma$ will rule out $J = 1$.

2.7 Parity of the Higgs

The CP property of the Higgs can best be tested in the $\gamma\gamma$ option [20]. For linearly polarized photons, an even-parity Higgs is produced when the photons have parallel spins, whereas an odd-parity Higgs can be produced when the photons have spins perpendicular to each other.

3. Search for new physics at the linear collider

3.1 Anomalous top couplings in continuum pair production

Anomalous top couplings to γ , like anomalous magnetic and electric dipole moments, would give evidence for beyond SM effects. Analogous dipole couplings to Z , called weak dipole couplings, are also possible. By suitable choice of angular or energy asymmetries, a sensitivity of $10^{-3} \times e/m_t$ is possible for anomalous dipole couplings, with longitudinally polarized beams [21,22]. It is also possible to study anomalous couplings to γ at a $\gamma\gamma$ collider [23–25].

3.2 Higgs in extensions of SM

The simplest extension of the Higgs sector is a two-Higgs doublet model. MSSM is a special case, with constrained couplings. With two Higgs doublets, the spectrum

consists of five scalars: H, h, A (neutral), H^\pm (charged). When there is no CP violation, H, h have CP=+, A has CP=-. If there is CP violation, there is mixing among H, h and A to give mass eigenstates H_1, H_2, H_3 which have no definite CP.

3.2.1 Higgs spectrum in MSSM

In MSSM at tree level, there are only two independent parameters because of the relations:

$$m_h \leq m_Z, \quad m_A \leq m_H, \quad m_{H^\pm}^2 = m_A^2 + m_W^2, \quad m_h^2 + m_H^2 = m_A^2 + m_Z^2. \quad (5)$$

Radiative corrections change these relations. A recent analysis, including full one-loop corrections and the two-loop corrections controlled by α_s and the Yukawa couplings of the third generation fermions gives an upper bound $m_h \lesssim 152$ GeV [26].

3.2.2 Higgs production in MSSM

The CP-even Higgses H, h are easily observable through Higgsstrahlung

$$e^+e^- \rightarrow Z + H, h \quad (6)$$

or WW, ZZ fusion,

$$e^+e^- \rightarrow \nu\bar{\nu} + H, h, \quad e^+e^- \rightarrow e^+e^- + H, h. \quad (7)$$

They can also be produced associated with the CP-odd A :

$$e^+e^- \rightarrow A + H, h. \quad (8)$$

The charged Higgs H^\pm can be pair produced:

$$e^+e^- \rightarrow H^+H^-. \quad (9)$$

Figure 7 from [11] shows examples of $e^+e^- \rightarrow Z + h, H$ and $e^+e^- \rightarrow A + h, H$ production cross-sections in the MSSM as functions of the respective Higgs masses for selected values of \sqrt{s} and $\tan\beta$.

3.2.3 Decay of MSSM Higgs

Branching ratios of the lightest neutral Higgs differ from those in SM. Precision measurements can give indirect evidence for SUSY. $R \equiv \Gamma(h \rightarrow b\bar{b})/\Gamma(h \rightarrow \tau\bar{\tau})$ is sensitive to parameters of MSSM. This is shown in figure 8, taken from [27]. The inner band gives 5% experimental uncertainty. For large $\tan\beta$, it is sensitive to $m_A \leq 600$ GeV for $\sqrt{s} = 350$ GeV and $L = 1000$ fb $^{-1}$.

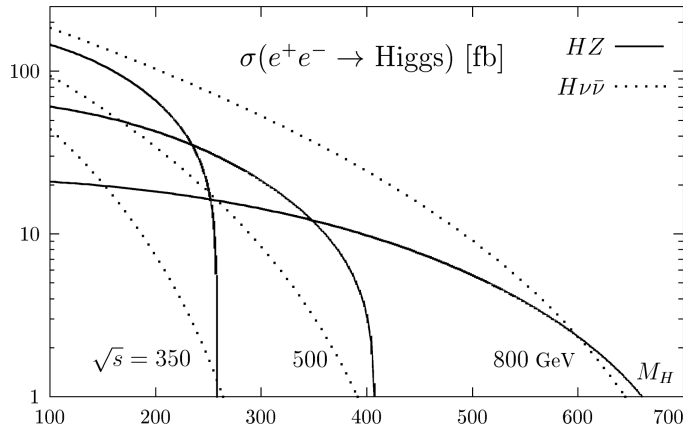


Figure 7. Production cross-sections of the neutral Higgs bosons in the MSSM at $\sqrt{s} = 350$ GeV in Higgsstrahlung and pair production processes for $\tan\beta = 3$ and 30 (from [11]).

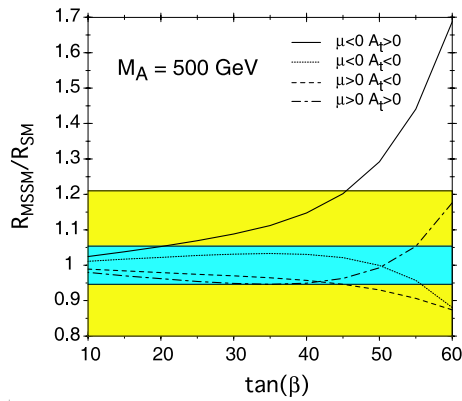


Figure 8. Deviation of the ratio $R \equiv \Gamma(h \rightarrow b\bar{b})/\Gamma(h^0 \rightarrow \tau\bar{\tau})$ from the SM prediction. The expected experimental uncertainty, $\sim 5\%$, is given by the inner bands (from [27]).

3.3 Search for supersymmetry at the linear collider

Supersymmetric extension of SM is the most theoretically motivated extension of SM. Supersymmetry is a symmetry of space–time that relates fermions and bosons. It associates with every known particle a new particle differing in spin by 1/2. These new particles are collectively known as ‘sparticles’. Supersymmetry relates the couplings of the new particles to those of known particles. This leads to predictions for production and decay rates of sparticles in terms of their masses. Supersymmetry breaking leads to mass splitting while preserving coupling constant relations.

Observing new particles associated with supersymmetry is a major goal of both LHC and ILC. At hadron colliders, all kinematically allowed sparticles are produced together. It is difficult to disentangle the pattern of sparticle masses and couplings.

On the other hand, a lepton collider which can change the cm energy can explore spectrum of sparticles systematically. Scalar sparticles associated with leptons are particularly difficult to observe at hadron colliders.

3.3.1 Goals for the study of supersymmetry

The goals for the study of supersymmetry would be to discover all the predicted sparticles, to measure the sparticle quantum numbers, to measure their masses and to measure the sparticle couplings to establish supersymmetry. In addition, the above measurements should be able to unravel the supersymmetry breaking scheme.

3.3.2 Supersymmetric partners

In supersymmetric theories, there is a new scalar partner for each chiral fermion. Each massive fermion has two scalar partners, labelled with suffixes L and R. In broken supersymmetry, these two partners can have different masses. Each gauge boson has a spin-1/2 partner ('gaugino'). In $SU(3) \times SU(2) \times U(1)$ these have masses denoted by M_3, M_2, M_1 corresponding to the group factors. Higgs bosons have spin-1/2 partners called higgsinos. Charged gauginos and higgsinos mix to give charginos $\tilde{\chi}_i^\pm$, $i = 1, 2$. Neutral gauginos and higgsinos mix to give neutralinos $\tilde{\chi}_i^0$, $i = 1, \dots, 4$.

3.3.3 R parity and LSP

The most popular class of supersymmetric models has R parity, a discrete symmetry imposed to prevent violation of lepton and baryon numbers. Because of R parity, supersymmetric particles are always produced in pairs. The lightest supersymmetric particle (LSP) is stable. LSP is usually assumed to be the lightest neutralino. LSP is also a viable candidate to explain dark matter in the Universe. ILC would be useful to test the candidacy of such a dark matter candidate by measuring its properties in detail [28].

3.3.4 Observation of sleptons

Scalar partners of leptons (sleptons \tilde{l}^\pm) can be produced through s -channel γ and Z exchange

$$e^+e^- \rightarrow \gamma, \quad Z \rightarrow \tilde{l}^+\tilde{l}^-. \quad (10)$$

Selectron pair production has an additional t -channel contribution from neutralino exchange. A slepton decays into a neutralino or chargino:

$$\tilde{l}^\pm \rightarrow \tilde{\chi}^0 l^\pm, \tilde{\chi}^\pm \nu_l. \quad (11)$$

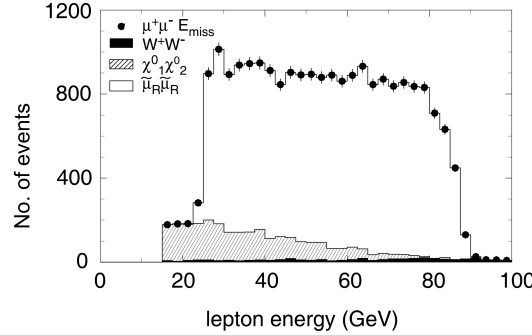


Figure 9. Signal from $e^+e^- \rightarrow \tilde{\mu}_R^+ \tilde{\mu}_R^- \rightarrow \mu^+ \mu^- \tilde{\chi}_1^0 \tilde{\chi}_1^0$ and the dominant backgrounds for $m_{\tilde{\mu}_R} = 132$ GeV and $m_{\tilde{\chi}_1^0} = 71.9$ GeV, $\sqrt{s} = 320$ GeV, and an integrated luminosity of $L = 160 \text{ fb}^{-1}$ (from [29]).

If the slepton decays to an LSP ($\tilde{\chi}_1^0$), the chain is

$$e^+e^- \rightarrow \tilde{l}^+ \tilde{l}^- \rightarrow l^+ l^- \tilde{\chi}_1^0 \tilde{\chi}_1^0. \quad (12)$$

The momentum of leptons is precisely measured, whereas neutralinos give missing transverse momentum.

The energy distribution of decay leptons is directly related to slepton and neutralino masses:

$$m_l^2 = \frac{s E_{\min} E_{\max}}{(E_{\min} + E_{\max})^2}; \quad 1 - \frac{m_{\tilde{\chi}_1^0}^2}{m_{\tilde{l}}^2} = \frac{2(E_{\min} + E_{\max})}{\sqrt{s}}. \quad (13)$$

The end-points E_{\min} , E_{\max} afford a measurement of slepton masses. The end-points of the lepton energy spectrum can be clearly seen in figure 9 [29]. The situation is more complicated in the case of $\tilde{\tau}$ sleptons due to the escaping neutrinos from τ decay. If the neutralino mass is known from smuon decay, the shape can be used to determine the stau mass. The dominant background is from $e^+e^- \rightarrow W^+W^- \rightarrow l^+ l'^- \nu_l \bar{\nu}_{l'}$. However, it is strongly peaked in the forward direction. It can therefore be reduced by an angular cut. The background can also be reduced by the use of polarized beams ($e_R^- e_L^+$).

Slepton masses can also be measured precisely from threshold energy scans, independent of the decay pattern. Because sleptons are scalars, threshold energy dependence scales like β^3 as compared to β dependence for fermion pairs. The absolute cross-section for slepton pair production measures the slepton couplings to 1–2% accuracy.

3.3.5 Charginos and neutralinos

Charginos and neutralinos are pair produced:

$$e^+e^- \rightarrow \tilde{\chi}_i^\pm \tilde{\chi}_i^\mp, \quad i = 1, 2; \quad (14)$$

Table 2. Sparticle masses and their expected precision for the SPS1a parameters and for the case of supersymmetry breaking with universal masses (mSUGRA scenario) (adapted from [30]).

	m	LHC	ILC	LHC+ILC		m	LHC	ILC	LHC+ILC
h	111.6	0.25	0.05	0.05	H	399.6		1.5	1.5
A	399.1		1.5	1.5	H^+	407.1		1.5	1.5
χ_1^0	97.03	4.8	0.05	0.05	χ_2^0	182.9	4.7	1.2	0.08
χ_3^0	349.2		4.0	4.0	χ_4^0	370.3	5.1	4.0	2.3
χ_1^\pm	182.3		0.55	0.55	χ_2^\pm	370.6		3.0	3.0
\tilde{e}_1	144.9	4.8	0.05	0.05	\tilde{e}_2	204.2	5.0	0.2	0.2
$\tilde{\mu}_1$	144.9	4.8	0.2	0.2	$\tilde{\mu}_2$	204.2	5.0	0.5	0.5
$\tilde{\tau}_1$	135.5	6.5	0.3	0.3	$\tilde{\tau}_2$	207.9		1.1	1.1
$\tilde{\nu}_e$	188.2		1.2	1.2					

$$e^+e^- \rightarrow \tilde{\chi}_i^0 \tilde{\chi}_i^0, \quad i = 1, 4. \tag{15}$$

Chargino production occurs through s -channel Z exchange and t -channel sneutrino exchange. The lightest chargino decays according to $\tilde{\chi}_1^\pm \rightarrow l^\pm \nu_l \tilde{\chi}_1^0$ either via intermediate W^\pm or via slepton. The dominant background is WW and ZZ production, which can be minimized using beam polarization. The chargino mass can be measured through the kinematic end-points of the decay products and through a threshold scan.

The second lightest neutralino decays according to $\tilde{\chi}_2^0 \rightarrow l^+ l^- \tilde{\chi}_1^0$ either via Z or via a slepton. The energy spectrum of the di-lepton system can be used to determine the masses of the primary and secondary neutralino, as in the case of slepton. $\tilde{\chi}_2^0$'s are also produced in decay chains. One can get a precise mass difference $\Delta m(\tilde{\chi}_2^0 - \tilde{\chi}_1^0)$ from the upper edge of the di-lepton mass spectrum. Charginos with the decay $\tilde{\chi}_1^\pm \rightarrow q\bar{q}' \tilde{\chi}_1^0$ give $\Delta m(\tilde{\chi}_1^\pm - \chi_1^0)$.

To give an idea of the precision of mass determination at ILC, sparticle masses and their expected precision for the point in parameter space known as SPS1a and for the case of supersymmetry breaking with universal masses (mSUGRA scenario) are shown in table 2.

3.3.6 SUSY with CP violation

There can be complex phases in various mass matrices in MSSM. This can lead to observable effects like electric dipole moments of fermions, which, due to the existing experimental limits, constrain the parameters of the theory. In addition, the presence of phases can affect the determination of the range of MSSM parameters from experimental information on even CP-conserving processes. In [31] production and decays of the third generation sfermions in the MSSM with complex parameters have been analysed. In a large region of the MSSM parameter space the branching ratios of these sfermions show a strong phase dependence. This could

have an important impact on the search for third generation sfermions at a future linear collider and on the determination of the supersymmetric parameters. CP violation can be studied in T-odd asymmetries in slepton, chargino and neutralino sectors which can arise even at tree level [32,33]. CP violation can also feed into the Higgs sector at higher orders. Thus, the Higgs states which are mass eigenstates are no longer eigenstates of CP [34]. A CP-violating Higgs sector can be studied also through the $\gamma\gamma$ option [35,36].

4. Theories with extra dimensions at the linear collider

In recent times, theories with extra dimensions have seen revived interest because of the possibility that an effective Planck scale can exist at TeV energy in such theories. There are three classes of extra-dimension models, differing from each other in the geometry of various fields. They have different experimental signatures. The common feature of all such models is the presence of closely spaced excitations extending into the TeV mass range and particles with spin-2. These are well-suited for study in e^+e^- collisions at the highest possible energies. Moreover, it has been proposed that the e^-e^- , $e^-\gamma$, and $\gamma\gamma$ options and the possibility of transverse polarization can be used to differentiate extra-dimension models.

4.1 The ADD model

In the original extra dimensions model in the recent context, the so-called ADD model due to Arkani-Hamed, Dimopoulos, and Dvali [37], SM fields are confined to a 1+3-dimensional brane. Gravity propagates in the ‘bulk’ of the other dimensions. Gravity is strong in the bulk, but only a fraction is felt on the brane. The relation between the Planck scale M_{Planck} and the compactification radius R is given, for d extra dimensions, by

$$M_{\text{Planck}}^2 \sim M_{\text{brane}}^{d+2} R^d, \quad (16)$$

where M_{brane} is the effective Planck mass scale on the 3-brane where SM lives. The effective Planck mass can be tuned to the TeV scale. For $d = 2$, R is on the order of a millimeter.

There is a tower of excited Kaluza–Klein (KK) graviton states which couple weakly to SM particles. In e^+e^- collisions the experimental signature for the model is missing energy in SM processes by radiation of a KK graviton from SM particles [38], or a change in the rate and angular distribution of pair production by virtue of the graviton propagator [39]. One signature of the first kind is missing energy in $e^+e^- \rightarrow \gamma + \text{missing energy}$ [40]. Another is a radiated graviton in Bhabha scattering [41]. Clean measurement of the angular distribution of final states in $\gamma + \text{missing energy}$ would distinguish the ADD model from a scenario where the missing energy is from extra neutrinos or superpartners.

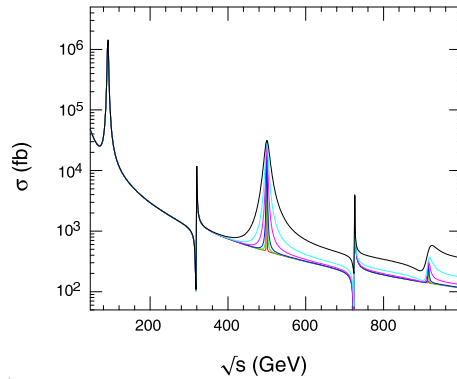


Figure 10. The cross-section for the production of a graviton and neutral gauge KK excitations in e^+e^- as a function of the c.m. energy \sqrt{s} for a model having first KK excitation at 500 GeV. The different curves correspond to various values of $\kappa/\bar{M}_{\text{Planck}}$ (from [43]).

4.2 Randall–Sundrum model

The Randall–Sundrum (RS) model allows for a brane having a TeV scale without large compactification radius of extra dimensions [42]. There is one extra dimension and two branes, one with an effective Planck mass at TeV scale and the other at the Planck scale. A scalar field in the bulk keeps the branes the proper distance apart. This results in a warp factor $e^{-\pi\kappa R}$ for the space–time metric, where κ is the curvature of fifth dimension and R is the compactification scale. A TeV scale on the low-energy brane is achieved if $\kappa R \sim 12$. Graviton masses are of electroweak scale, and there is a series of KK gravitons. The masses of the KK excitations of the gravitons are $M_n = \zeta_n m_0$, where $m_0 = \kappa e^{-\pi\kappa R}$ and ζ_n are zeroes of the Bessel function [43]. Other schemes lead to different mass spacings. It is more useful to consider model parameters as m_0 and $c_0 = \kappa/\bar{M}_{\text{Planck}}$, the effective coupling. The gravitons have weak strength and decay into pairs of SM particles with a width dependent on c_0 . Figure 10, taken from [43], shows the cross-section for the e^+e^- production of graviton and neutral gauge KK excitations for a model having the first KK excitation at 500 GeV. The series of curves represents various values of $\kappa/\bar{M}_{\text{Planck}}$. The gravitons have weak strength and decay into pairs of standard model particles with a width dependent on c_0 . Thus, because of the good resolution of an e^+e^- collider, the excitations can be easily observed.

The difference between ADD and RS in the production of single photons vs. dimuons at $\sqrt{s} = 2$ TeV is shown in figure 11, taken from [44]. It is thus possible to distinguish between the two scenarios.

4.3 Universal extra dimensions

In the model with universal extra dimensions (UED), all SM fields live in the extra-dimensional bulk. Thus, all SM particles have KK excitations [45]. In UED models,

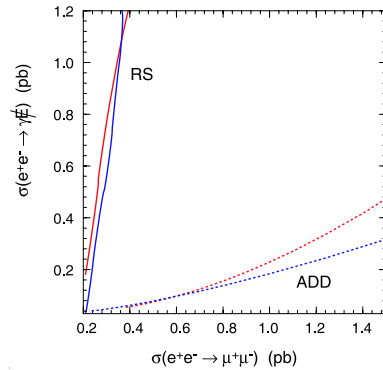


Figure 11. Cross-sections for the production of single photons and of dimuons at $\sqrt{s} = 2$ TeV are plotted against each other. ADD lines are for extra dimensions of 3 and 6. The RS curves are for $m_0 = 200$ and 400 GeV (from [44]).

there is a conservation of KK mode number. Thus, at lowest order, excited particles are produced in pairs. The lightest KK particle is the photon with $n = 0$. This model is similar to SUSY to the extent that every SM particle has a tower of KK-partners, even though these partners have the same spin. Determining whether one is seeing UED or SUSY will require excellent determination of angular distributions.

5. Models with extra Z at the linear collider

There are several models with extra neutral gauge boson Z' , as for example, grand unification (E_6 ξ models), left-right symmetry [30,46–48] KK excitations of γ and Z [49] and little Higgs model(s) [50].

ILC can make precision measurements of various observables in $e^+e^- \rightarrow f\bar{f}$: $\sigma_0 \equiv \sigma(e^+e^- \rightarrow \mu^+\mu^-)$, $R^{\text{had}} \equiv \sigma^{\text{had}}/\sigma_0$, A_{FB}^l , A_{LR}^l , $A_{\text{LR}}^{\text{had}}$, A_{pol}^τ , and $A_{\text{FB}}^f(\text{pol})$. Here the notation is standard; the subscript ‘had’ refers to hadronic cross-sections, ‘FB’ refers to ‘forward-backward’, ‘LR’ to ‘left-right’ (asymmetry) in the context of longitudinal polarization of beams, and ‘pol’ to the polarized beams.

Beam polarization with P_{e^-} and P_{e^+} of opposite signs helps to enhance cross-section, as seen from eq. (1). With $\sqrt{s} = 500$ GeV, $L = 1 \text{ ab}^{-1}$, $P_{e^-} = 0.8$, $P_{e^+} = 0.6$, $m_{Z'}$ up to 2–3 TeV can be probed at 95% CL. It is found that there is an ambiguity if only leptonic final states are used [51]. It is resolved if hadronic states are included in addition to leptonic states [52]. In any case beam polarization plays an important role [52].

6. Conclusions

To conclude, a description has been given of various physics capabilities of an e^+e^- linear collider and its options. It is clear that a lot of precision information within

SM and beyond would become available with such a collider. With the determined effort of the international high energy physics community, ILC seems certain to become a reality.

References

- [1] American Linear Collider Working Group: J Bagger *et al*, arXiv:hep-ex/0007022
ACFA Linear Collider Working Group: K Abe *et al*, arXiv:hep-ph/0109166
ECFA/DESY LC Physics Working Group: J A Aguilar-Saavedra *et al*, arXiv:hep-ph/0106315
A Bartl and S Hesselbach, *Pramana – J. Phys.* **63**, 1101 (2004); arXiv:hep-ph/0407178
S Dawson and M Oreglia, *Ann. Rev. Nucl. Part. Sci.* **54**, 269 (2004); arXiv:hep-ph/0403015
- [2] G A Moortgat-Pick *et al*, arXiv:hep-ph/0507011
- [3] I F Ginzburg, G L Kotkin, V G Serbo and V I Telnov, *Nucl. Instrum. Methods* **205**, 47 (1983)
- [4] I F Ginzburg, G L Kotkin, S L Panfil, V G Serbo and V I Telnov, *Nucl. Instrum. Methods* **A219**, 5 (1984)
V I Telnov, *Nucl. Instrum. Methods* **A355**, 3 (1995)
- [5] W Menges, LC-PHSM-2001-022
- [6] D Choudhury and S D Rindani, *Phys. Lett.* **B335**, 198 (1994); arXiv:hep-ph/9405242
B Ananthanarayan, S D Rindani, R K Singh and A Bartl, *Phys. Lett.* **B593**, 95 (2004); Erratum, *ibid* **B608**, 274 (2005); arXiv:hep-ph/0404106
- [7] A H Hoang, A V Manohar, I W Stewart and T Teubner, *Phys. Rev.* **D65**, 014014 (2002); arXiv:hep-ph/0107144
- [8] A H Hoang, *Phys. Rev.* **D69**, 034009 (2004); arXiv:hep-ph/0307376
- [9] A H Hoang and T Teubner, *Phys. Rev.* **D60**, 114027 (1999); arXiv:hep-ph/9904468
A H Hoang, Z Ligeti and A V Manohar, *Phys. Rev. Lett.* **82**, 277 (1999); arXiv:hep-ph/9809423
- [10] M Martinez and R Miquel, *Eur. Phys. J.* **C27**, 49 (2003); arXiv:hep-ph/0207315
- [11] A Djouadi, *Pramana – J. Phys.* **60**, 215 (2003); arXiv:hep-ph/0205248
- [12] T Kuhl, <http://www-flc.desy.de/ecfa-higgs/montpellier/kuhl-montpellier.pdf>
- [13] M Battaglia and A De Roeck, in *Proc. of the APS/DPF/DPB Summer Study on the Future of Particle Physics (Snowmass 2001)* edited by N Graf, eConf **C010630**, E3066 (2001); arXiv:hep-ph/0111307
- [14] A Juste and G Merino, arXiv:hep-ph/9910301
A Gay, arXiv:hep-ph/0604034
H Baer, S Dawson and L Reina, *Phys. Rev.* **D61**, 013002 (2000); arXiv:hep-ph/9906419
- [15] U Baur, T Plehn and D L Rainwater, *Phys. Rev.* **D68**, 033001 (2003); arXiv:hep-ph/0304015
C Castanier, P Gay, P Lutz and J Orloff, arXiv:hep-ex/0101028
M Battaglia, E Boos and W M Yao, in *Proc. of the APS/DPF/DPB Summer Study on the Future of Particle Physics (Snowmass 2001)* edited by N Graf, eConf **C010630**, E3016 (2001); arXiv:hep-ph/0111276
- [16] A Djouadi, W Kilian, M Muhlleitner and P M Zerwas, *Euro. Phys. J.* **C10**, 27 (1999); arXiv:hep-ph/9903229

- [17] D J Miller, S Y Choi, B Eberle, M M Muhlleitner and P M Zerwas, *Phys. Lett.* **B505**, 149 (2001); arXiv:hep-ph/0102023
- [18] M T Dova, P Garcia-Abia and W Lohmann, arXiv:hep-ph/0302113.
- [19] S Y Choi, D J Miller, M M Muhlleitner and P M Zerwas, *Phys. Lett.* **B553**, 61 (2003); arXiv:hep-ph/0210077
- [20] B Grzadkowski and J F Gunion, *Phys. Lett.* **B294**, 361 (1992); arXiv:hep-ph/9206262
- [21] S D Rindani, *Pramana – J. Phys.* **61**, 33 (2003); arXiv:hep-ph/0304046
P Poulou and S D Rindani, *Phys. Rev.* **D57**, 5444 (1998); Erratum, *ibid.* **D61**, 119902 (2000); arXiv:hep-ph/9709225; *Phys. Lett.* **B383**, 212 (1996); arXiv:hep-ph/9606356; *Phys. Rev.* **D54**, 4326 (1996); Erratum, *ibid.* **D61**, 119901 (2000); arXiv:hep-ph/9509299; *Phys. Lett.* **B349**, 379 (1995); arXiv:hep-ph/9410357
F Cuypers and S D Rindani, *Phys. Lett.* **B343**, 333 (1995); arXiv:hep-ph/9409243
- [22] D Atwood, S Bar-Shalom, G Eilam and A Soni, *Phys. Rep.* **347**, 1 (2001); arXiv:hep-ph/0006032
- [23] P Poulou and S D Rindani, *Phys. Rev.* **D57**, 5444 (1998); Erratum, *ibid.* **D61**, 119902 (2000); arXiv:hep-ph/9709225
- [24] M S Baek, S Y Choi and C S Kim, *Phys. Rev.* **D56**, 6835 (1997); arXiv:hep-ph/9704312
S Y Choi and K Hagiwara, *Phys. Lett.* **B359**, 369 (1995); arXiv:hep-ph/9506430
- [25] B Grzadkowski, Z Hioki, K Ohkuma and J Wudka, *Acta Phys. Polon.* **B36**, 3531 (2005); arXiv:hep-ph/0511038
B Grzadkowski, Z Hioki, K Ohkuma and J Wudka, *Nucl. Phys.* **B689**, 108 (2004); arXiv:hep-ph/0310159
- [26] B C Allanach, A Djouadi, J L Kneur, W Porod and P Slavich, *J. High Energy Phys.* **0409**, 044 (2004); arXiv:hep-ph/0406166
- [27] J Guasch, W Hollik and S Penaranda, arXiv:hep-ph/0307012; *Phys. Lett.* **B515**, 367 (2001); arXiv:hep-ph/0106027
- [28] S Kraml, these proceedings
- [29] H U Martyn and G A Blair, arXiv:hep-ph/9910416.
- [30] LHC/LC Study Group: G Weiglein *et al*, arXiv:hep-ph/0410364
- [31] A Bartl, K Hidaka, T Kernreiter and W Porod, *Phys. Lett.* **B538**, 137 (2002); arXiv:hep-ph/0204071; *Phys. Rev.* **D66**, 115009 (2002); arXiv:hep-ph/0207186
A Bartl, S Hesselbach, K Hidaka, T Kernreiter and W Porod, arXiv:hep-ph/0306281; *Phys. Lett.* **B573**, 153 (2003); arXiv:hep-ph/0307317; arXiv:hep-ph/0311338
- [32] S Y Choi, H S Song and W Y Song, *Phys. Rev.* **D61**, 075004 (2000); arXiv:hep-ph/9907474
- [33] Y Kizukuri and N Oshimo, *Phys. Lett.* **B249**, 449 (1990)
A Bartl, H Fraas, S Hesselbach, K Hohenwarter-Sodek and G Moortgat-Pick, arXiv:hep-ph/0406190
A Bartl, H Fraas, O Kittel and W Majerotto, *Phys. Rev.* **D69**, 035007 (2004); arXiv:hep-ph/0308141
A Bartl, H Fraas, O Kittel and W Majerotto, arXiv:hep-ph/0402016
- [34] A Pilaftsis, *Phys. Lett.* **B435**, 88 (1998); arXiv:hep-ph/9805373
A Pilaftsis and C E M Wagner, *Nucl. Phys.* **B553**, 3 (1999); arXiv:hep-ph/9902371
- [35] R M Godbole, S D Rindani and R K Singh, *Phys. Rev.* **D67**, 095009 (2003); Erratum, *ibid.* **D71**, 039902 (2005)
- [36] E Asakawa, S Y Choi, K Hagiwara and J S Lee, *Phys. Rev.* **D62**, 115005 (2000); arXiv:hep-ph/0005313
J R Ellis, J S Lee and A Pilaftsis, *Nucl. Phys.* **B718**, 247 (2005); arXiv:hep-ph/0411379

- [37] N Arkani-Hamed, S Dimopoulos and G R Dvali, *Phys. Lett.* **B429**, 263 (1998); arXiv:hep-ph/9803315; *Phys. Rev.* **D59**, 086004 (1999); arXiv:hep-ph/9807344
I Antoniadis, N Arkani-Hamed, S Dimopoulos and G R Dvali, *Phys. Lett.* **B436**, 257 (1998); arXiv:hep-ph/9804398
- [38] O J P Eboli, M B Magro, P Mathews and P G Mercadante, *Phys. Rev.* **D64**, 035005 (2001); arXiv:hep-ph/0103053
- [39] G F Giudice, R Rattazzi and J D Wells, *Nucl. Phys.* **B544**, 3 (1999); arXiv:hep-ph/9811291
T Han, J D Lykken and R J Zhang, *Phys. Rev.* **D59**, 105006 (1999); arXiv:hep-ph/9811350
K Agashe and N G Deshpande, *Phys. Lett.* **B456**, 60 (1999); arXiv:hep-ph/9902263
K M Cheung and G Landsberg, *Phys. Rev.* **D65**, 076003 (2002); arXiv:hep-ph/0110346
- [40] E A Mirabelli, M Perelstein and M E Peskin, *Phys. Rev. Lett.* **82**, 2236 (1999); arXiv:hep-ph/9811337
S Gopalakrishna, M Perelstein and J D Wells, in *Proc. of the APS/DPF/DPB Summer Study on the Future of Particle Physics (Snowmass 2001)* edited by N Graf, eConf **C010630**, P311 (2001); arXiv:hep-ph/0110339
- [41] S Dutta, P Konar, B Mukhopadhyaya and S Raychaudhuri, *Phys. Rev.* **D68**, 095005 (2003); arXiv:hep-ph/0307117
- [42] L Randall and R Sundrum, *Phys. Rev. Lett.* **83**, 4690 (1999); arXiv:hep-th/9906064
- [43] H Davoudiasl, J L Hewett and T G Rizzo, *Phys. Rev.* **D63**, 075004 (2001); arXiv:hep-ph/0006041
- [44] S K Rai and S Raychaudhuri, *J. High Energy Phys.* **0310**, 020 (2003); arXiv:hep-ph/0307096
- [45] T Appelquist and B A Dobrescu, *Phys. Lett.* **B516**, 85 (2001); arXiv:hep-ph/0106140
- [46] S Capstick and S Godfrey, *Phys. Rev.* **D37**, 2466 (1988)
S Godfrey, *Phys. Rev.* **D51**, 1402 (1995); arXiv:hep-ph/9411237
- [47] A Leike, *Phys. Rep.* **317**, 143 (1999); arXiv:hep-ph/9805494
M Cvetič and S Godfrey, arXiv:hep-ph/9504216
- [48] ECFA/DESY LC Physics Working Group: J A Aguilar-Saavedra *et al*, arXiv:hep-ph/0106315
- [49] T G Rizzo, eConf **C040802**, L013 (2004); arXiv:hep-ph/0409309
K Cheung, arXiv:hep-ph/0409028
- [50] N Arkani-Hamed, A G Cohen, E Katz and A E Nelson, *J. High Energy Phys.* **0207**, 034 (2002); arXiv:hep-ph/0206021
M Schmaltz, *J. High Energy Phys.* **0408**, 056 (2004); arXiv:hep-ph/0407143
M Schmaltz and D Tucker-Smith, *Ann. Rev. Nucl. Part. Sci.* **55**, 229 (2005); arXiv:hep-ph/0502182
T Han, H E Logan, B McElrath and L T Wang, *Phys. Rev.* **D67**, 095004 (2003); arXiv:hep-ph/0301040
T Han, H E Logan and L T Wang, *J. High Energy Phys.* **0601**, 099 (2006); arXiv:hep-ph/0506313
- [51] S. Riemann in ref. [48]
- [52] S Godfrey, P Kalyniak and A Tomkins, arXiv:hep-ph/0511335